Analysis of On-Body Transponders Based on Frequency Selective Surfaces

Javier Lorenzo*, Antonio Lazaro, David Girbau, Ramon Villarino, and Ernest Gil

Abstract—This paper proposes a backscattering communication technique based on modulated frequency selective surfaces (FSS) for wearable applications. The FSS is composed of dipoles loaded with varactor diodes to modulate the backscatter response, in order to separate it from the clutter. The paper describes the effect in the transponder response according to the number of dipoles, the separation between them and the effect produced when FSS is placed on-body. An analysis based on simulations of several cases and experimental results is provided.

1. INTRODUCTION

The interest in wearable technology for wireless body area network (WBAN) is growing rapidly in the recent years. Wearable devices can integrate sensors for different fields such as medical, assisted living, sports and entertainment [1]. However, some challenges should be addressed for practical WBAN applications. These include low-cost and also continuous monitoring, which determine the energy required and the battery lifetime. The WBAN devices must be wearable, lightweight and non-intrusive. The wireless link should be robust in the user environment. Active wireless devices are often proposed for wireless communications in WBAN. These networks are often based on commercial transceivers such as Zigbee (IEEE 802.15.4) or Bluetooth devices or WIFI (IEEE 802.11) at 2.45 GHz ISM band [2, 3]. An important part of the energy is needed for the transmission. Therefore, the battery lifetime depends on the time interval between transmissions. The worst case happens in real-time applications, where continuous monitoring is required. Different energy harvesting technologies are researched in order to increase the autonomy of the wearable devices [4, 5]. However, these techniques are often not compatible with active wireless devices that are continuously real-time monitoring. On the opposite side to the active devices, wearable passive UHF Radio-Identification (RFID) sensors can be found, and they have been investigated at [6–8]. Passive tags take their energy from the RF interrogating signal. Therefore, the losses caused by the body reduce the power received by the tag, decreasing the read range with respect to the cases in which the tags work at free space. Special antenna designs compatible with wearable devices are needed, but the proximity of the body reduces their efficiency. On the other hand, Non-line-of-sight (NLOS) scenery due to the presence of body that blocks the signal can be considered. This fact and multipath propagation will make difficult to power up the tag. Several wearable antennas such as patch antennas or spacers to separate the antenna from the body have been reported in the literature [9]. Some of these problems can be relaxed if semi-passive or battery assisted tags (BAP) are employed. The main advantage of a semi-passive platform compared to active transceivers is related to its power consumption, which is generally determined by the current consumption of the digital core (microcontroller) and the sensors [10]. The cost of these tags when manufactured in large volumes is lower than wireless active sensors (e.g., using Bluetooth or Zigbee standards) and the battery lifetime

* Corresponding author: Antonio Lazaro (antonioramon.lazaro@urv.cat).

The authors are with the Department of Electronics, Electrics and Automatics Engineering, Universitat Rovira i Virgili (URV), Av. Països Catalans 26, Campus Sescelades, Tarragona 43007, Spain.

is considerable higher, which is translated on simple power circuits (e.g., rechargeable batteries and charging circuits are not required). However, the communication problems are not completely solved because they are based on backscattering. For example, reported read range on passive epidermal body is 0.8 m [11] and 0.5 m [12] when temperature-sensing microchips were included The main reason for this is the limitation on the uplink budget between the reader and the tag, since the passive RFID tags require a minimum received power to wake up its internal circuitry, given that the tag is fed from the rectified voltage from the incoming wave.

One important disadvantage in antennas for WBAN applications is the reduction of antennas efficiency due to the proximity of the body, which increases the losses. In addition, the presence of the body modifies the antenna's response, being a critical parameter in case of using narrow-band antennas such as patches. It means that sometimes the design requires spacers located between the antennas and the body or an increase of the height substrate. These techniques can make difficult the integration on wearable devices. In order to increase the read range for wearable semipassive tags, this work proposes the use of a modulated frequency selective surface (FSS). Using the proposed FSS, an increase of the tag thickness and multilayer designs are not required, facilitating its integration in wearable applications.

The FSS is periodic structures in each direction of the plane, and it acts as a filter. This filter property has been exploited in several applications [13]. In [14] the bandpass frequency can be modified using tuning devices such as varactors or PIN diodes. In previous works, the authors demonstrate the use of a transponder based on an FSS to reduce the interference from clutter reflections by changing its radar cross section (RCS) using the classic backscattering technique for RFID applications. The illumination signal is generated by readers based on FMCW radars at X band [15] or ultra-wide band (UWB) radars [16]. However, the effect of the materials attached to the transponder in terms of loss and detuning has not been considered, assuming the case of free space. The backscatter transponder is used to improve the read range for indoor localization or to mitigate disturbances caused by the multipath reflections [17].

A proof of the concept of frequency modulated transponder for on-body applications has recently been presented by the authors [18]. This work is a complementary work that addresses the study of the contribution of different parameters in the transponder design such as the number of elements of the FSS, influence of variations in the dielectric properties of the body and the separation between them in order to increase the power reflection, and also studies its bandwidth. The effect when the transponder is placed in high-loss materials such as the body is also considered here. The effect of the distance between the FSS and the body introduced by textile or rubber materials is also analyzed.

The paper is organized as follows. Section 2 summarizes the basic theory of the backscattered transponder described in [15, 18]. A description of the transponder design is performed and its behaviour is studied from electromagnetic simulations according to previous mentioned parameters. In Section 3, experimental results are provided as proof of concept. Finally, Section 4 draws the conclusions.

2. MODULATION THEORY AND FSS TRANSPONDER DESIGN

2.1. Modulation Theory

The modulation theory of FSS is summarized in this section, and it has been described in detail in previous works [15, 18]. Figure 1(a) shows a block diagram of the proposed system. It is composed by a reader and the transponder, which is in turn connected to a low-frequency generator (Agilent 33521A) that modulates its radar cross section. The transponder or tag (see Figure 2(a)) is based on an FSS with dipoles loaded with reverse biased varactors that are switched between 0 V and −3 V using a low-frequency generator. To demonstrate the concept, the reader is composed of a transmitter (frequency generator Rohde&Schwarz SMF100), and a receiver (spectrum analyzer Rohde&Schwarz FSP). In order to characterize the transponder, two wideband (1.5–4.5 GHz) antennas (GEOZONDAS AU-1.0G4.5GR) are connected to the transmitter and the receiver.

The generator transmits a continuous wave (CW) that illuminates the tag (X_T), which answers by modulating the backscattered field that can be studied from the fundamental antenna scattering theory [19, 20]. The backscattered field of the FSS can be split as a sum of two terms [15]: a structural mode and an antenna mode (also referred as tag mode), or in other words, a load-independent term
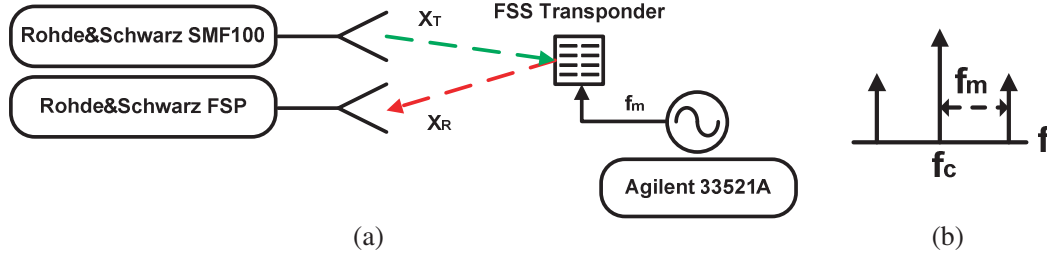
Figure 1. (a) Block diagram of the setup for experimental characterization. (b) Spectrum of the received signal.

and a load-dependent term, respectively:

$$\overline{E}_s(Z_L) = \overline{E}_{est} + \overline{E}_m \Gamma \tag{1}$$

where $E_S(Z_L)$ is the scattered field by the FSS when each element is loaded with the load Z_L, and E_{est} is the scattered field when the tag is connected to a reference load $Z_L = Z_a^*$, where Z_a is the FSS scan impedance [13]. Γ is the power reflection coefficient given by [19]: $\Gamma = (Z_L - Z_a^*)/(Z_L + Z_a)$. By switching the varactor diodes that load the dipoles of the FSS, the reflection coefficient is modulated. The reflection coefficient changes between Γ_{ON} when the diodes are biased at $0\,\mathrm{V}$ and Γ_{OFF} when the diodes are biased at $-3\,\mathrm{V}$. The reflection coefficient can be approximated by a square waveform of amplitude $\Delta\Gamma = \Gamma_{ON} - \Gamma_{OFF}$. This variation is mainly due to the change of the varactor capacitance between both states. It can be developed in a Fourier series [15]:

$$\Gamma(f) = \sum_{n=-\infty}^{+\infty} c_n \delta(f - (f_c + nf_m)) \tag{2}$$

where c_n are the Fourier coefficients; f_c is the input frequency of the incident signal that illuminates the tag; f_m is the inverse of the square waveform's period. Consequently, a modulation of the backscattered field is produced.

Figure 1(b) shows the spectrum of the received signal (X_R). A strong central peak can be observed at the illuminating carrier frequency, f_c. This component is due to the structural mode of the backscattered field, but it can be masked by the coupling signal between the transmitter's and receiver's antennas. The level of the coupling signal does not depend on distance. Therefore, it is difficult to distinguish the structural mode except at very short ranges. However, thanks to the FSSs' response modulation, a sideband appears at every f_m multiple, as it can be seen at the spectrum. The first spectral component (that corresponds to the Fourier terms at $n = \pm 1$) is be the most interesting since the levels of the rest of the harmonics are often bellow the noise floor of the receiver. This first spectral component can be used to send information from sensors, for example modulating their amplitude or frequency f_m. Analogue or digital modulation methods can be implemented depending on the application.

The amplitude of the sideband at $f_c \pm f_m$ is proportional to the differential RCS, RCS_{dif} [15]. It can be rewritten as the already known expression used in conventional RFID technology [20]:

$$RCS_{dif} = \lim_{r\to\infty} 4\pi r^2 \frac{\left|\overline{E}(Z_{L,ON}) - \overline{E}(Z_{L,OFF})\right|^2}{\left|\overline{E}_{in}\right|^2} = \lim_{r\to\infty} 4\pi r^2 \frac{\left|\overline{E}_m c_1\right|^2}{\left|\overline{E}_{in}\right|^2} = \frac{\lambda^2}{4\pi} G^2 \left|\Delta\Gamma\right|^2 m \tag{3}$$

where λ is the wavelength, G the tag's gain, and m a modulating factor ($m = |c_1|^2/|\Delta\Gamma|^2$). Therefore, the level of the received signal can be improved by increasing the number of elements (antennas) of the FSS or equivalently, its area.

2.2. Transponder Design and Simulations

FSSs are ideally infinite periodic structures, but due to the space limitations in wearable applications, the number of elements devices must be finite. Even if the FSS can be integrated in textile clothes or
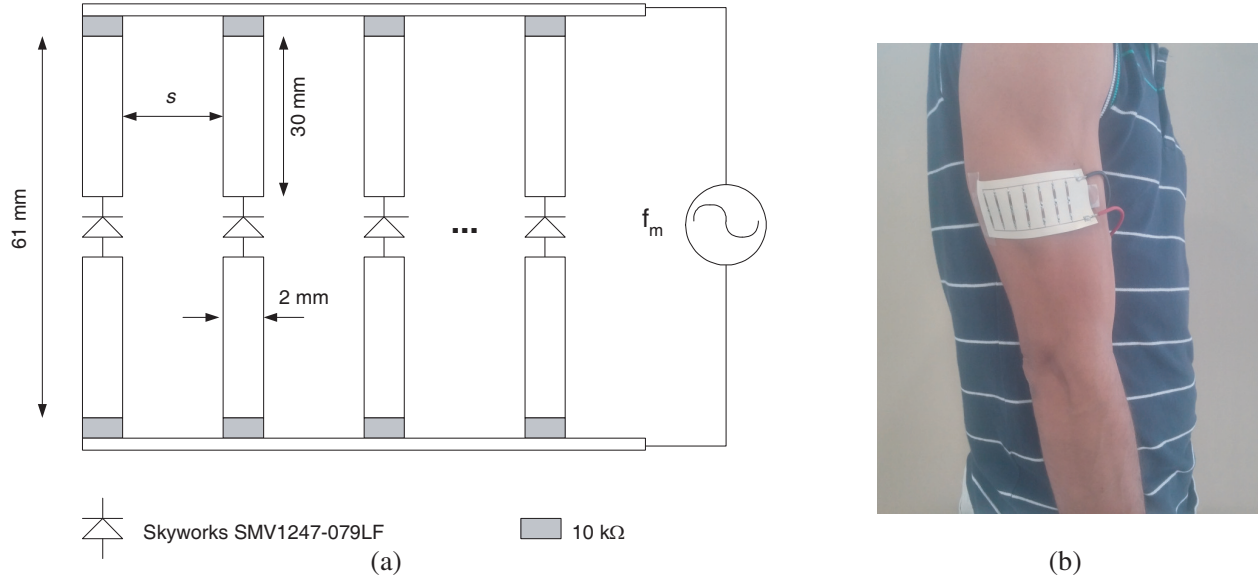
Figure 2. (a) FSS transponder basic schema used in the simulations and (b) prototype fabricated placed on the arm.

belts, and thus the area may be relatively large, a large number of elements (and diodes) might increase its cost. Therefore, the number of elements must be small, and consequently the influence of the number of elements must be studied.

Figure 2 shows a schema of a typical modulated FSS composed by the dipoles and bias network. The dipoles are loaded with low-cost silicon varactor diodes from Skyworks SMV1247-079LF. The length of the dipoles controls the passband of the FSS. Its value is 61 mm, and it is adjusted to operate on body at 2.45 GHz. The separation of dipoles (s) must be under $\lambda/2$ to avoid the grating modes [13]. In this work, a separation of $\lambda/4$ is considered. The effect of this parameter will be shown in next simulations. In order to avoid any undesired load effect of the bias lines, the diodes are biased using 10 kΩ at the end of the dipoles (acting as high impedance points), and the bias lines are orthogonal to the dipole orientation. The equivalent circuit of the diode is modelled by a lumped RLC series that is used as boundary condition in the HFSS simulations. From the manufacturer datasheet, the diode capacitance is 6.5 pF and 0.95 pF for $V = 0$ (ON state) and $V = -3$ V (OFF state), respectively. The parasitic inductance and resistance are 0.7 nH and 2 Ω, respectively.

The differential RCS can be evaluated using Eq. (3) from Ansoft HFSS simulations subtracting the backscattered field when a plane wave illuminates the structure for the two diode states (ON and OFF). For computational cost, it is not possible to simulate all the body; therefore, a small part of it is considered. It is assumed that the body reflects a large part of the power that contributes to the structural mode, which will be cancelled when the differential RCS is calculated in Eq. (3). In order to understand the influence of body loss, several scenarios have been considered. Figure 3 shows these scenarios: FSS on a free space, FSS printed on a substrate, FSS attached to the body and FSS close to the body spaced by a thin hard rubber and low permittivity layer. It is assumed that the FSS transponder will be attached on the arm in the final application.

2.2.1. Effect of Number of Dipoles in Free Space and on Thin Substrate

In order to investigate the effect of number of dipoles, the differential RCS for different numbers of dipoles has been simulated and is shown in Figure 4(a), including the diode model (two states) in free space (Figure 3(a)). It is observed that the increase in the number of dipoles produces an increase both in the differential RCS and in the bandwidth. For example, a bandwidth between 2 GHz and 3 GHz is achieved for 5 or more dipoles.

However, for wearable applications, the FSS must be manufactured over flexible substrates. The
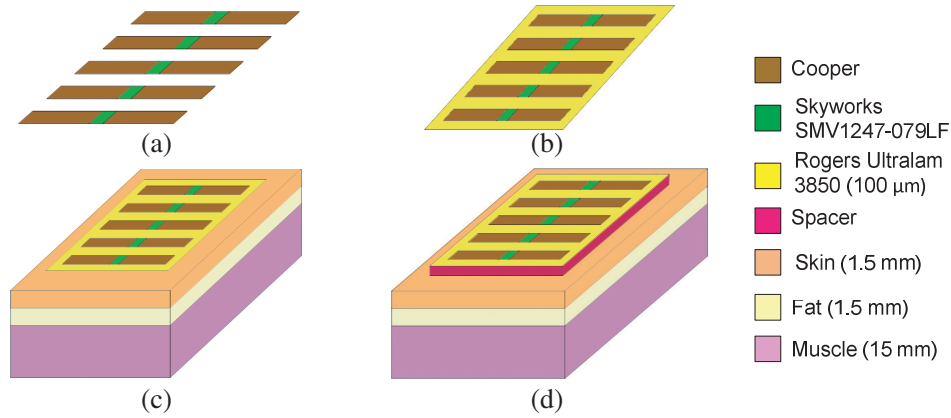
Figure 3. Structures simulated in HFSS: (a) dipoles in free space, (b) dipoles on substrate in free space, (c) FSS transponder placed on body model without spacer and (d) with different thickness of spacer.
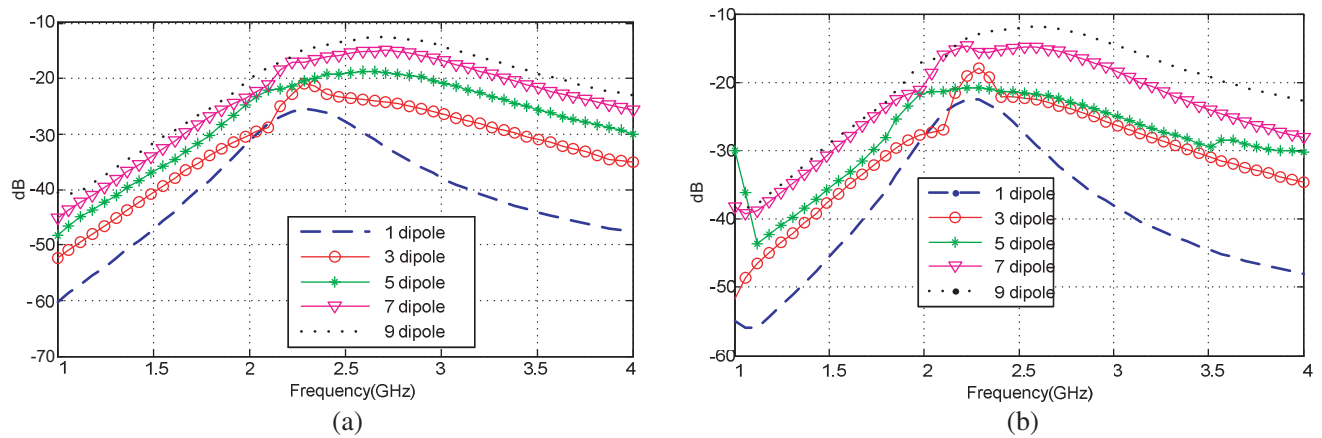

Figure 4. Comparison of FSS structure with different numbers of elements (a) in free space and (b) printer over a thin substrate.

influence of the thin low-loss substrate is expected to be small. This hypothesis is confirmed in Figure 4(b) where the FSS is printed on a Rogers Ultralam 3850 substrate ($\varepsilon_r = 3.14$, $\tan \delta = 0.0025$, thickness $100 \, \mu\text{m}$). A small reduction of the bandwidth and a small shift to lower frequency (due to the small increase in the effective permittivity) are observed in this case (Figure 4(b)) compared with the free space case (Figure 4(a)).

### 2.2.2. Influence of the Dipole Spacing

In order to improve the differential RCS of the FSS, simulations varying the separation between the dipoles (s) are carried out. Figure 5 compares the results for $s = \lambda/6$, $\lambda/5$ and $\lambda/4$. It is observed that when s decreases, the coupling between dipoles increases and the differential RCS decreases because the FSS area diminishes. In addition, the bandwidth also diminishes when the spacing decreases, and the central frequency is shifted. These effects are more significant considering a structure of 7 dipoles.

2.2.3. Influence of the Body

Figure 6 shows several simulations of the differential RCS when the FSS is placed on the body. Three cases are considered: FSS directly in contact with the body (Figure 3(c)), and separated with a low permittivity spacer of $2 \, \text{mm}$ and $4 \, \text{mm}$ thick (Figure 3(d)). Table 1 shows the thickness and electrical

Table 1. Dielectric properties of arm used in simulations.

Layer	Thickness (mm)	Relative Permittivity	Dissipation Loss Tangent
Skin	1.5	42.8	0.27
Fat	1.5	5.3	0.14
Muscle	15	53.6	0.24
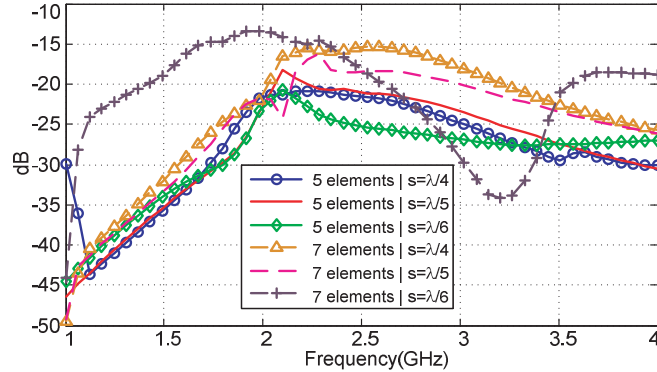
Figure 5. Return loss of a circular corrugated horn.

properties (relative permittivity and dissipation loss tangent) of the layers used to simulate the arm at 2.45 GHz, obtained from [22, 23].

It can be concluded from Figure 6 that the differential RCS decreases around 6–7 dB due to the loss introduced by the body compared with the results obtained in free space (Figures 4–5). This effect has also been reported on wearable antennas for UHF RFID [23]. The other effect that can be observed is the shift of the bandpass response to lower frequencies since the effective permittivity increases enormously due to the body. In a real scenario, the effects of the detuning can be overcome by reducing the length of dipoles. There are not significant differences for spacers higher than 2 mm. Therefore, the combination of large bandwidth and low sensitivity to the spacing is very interesting for wearable applications since the dielectric properties can change between persons or depend on the position where the tag is attached. The small spacing introduced by a bracelet that supports the FSS can be used to make variation independent from the change in the dielectric properties. The reduction on the differential RCS due to the body losses can be compensated by increasing the number of elements or using various rows of dipoles. Figure 7 depicts the differential RCS when being placed on the body and on free space for an FSS with 5 elements and an FSS with 10 elements distributed in two rows (five in each row). The frequency response practically does not change, and there is only an increase in the level due to the increase in the reflecting surface and the number of elements. In order to investigate the effect of these changes on the FSS performance, the effect of thickness of the fat layer (t) is investigated in Figure 8, which shows the differential RCS of an FSS of 5 elements as function of the thickness of fat layer (t). As reference, the simulation of FSS in free space is also shown. The effective permittivity decreases when the thickness of the fat layer increases, and as a consequence, the frequency response is slightly shifted to higher frequencies. However, as the frequency response of the FSS is quite flat around the resonance, the detuning effect is not very important. In conclusion, it can be expected that the FSS is robust in front of variations in the body locations (or the persons) where it will be attached. This robustness is analysed in the experimental results obtained in the next section.

3. EXPERIMENTAL RESULTS

According to the setup presented in Figure 1, some FSS transponders are characterized. The tag is modulated with a low-frequency generator (Agilent 33521A) at $f_m = 7$ kHz, 3 Vpp. A prototype with 7
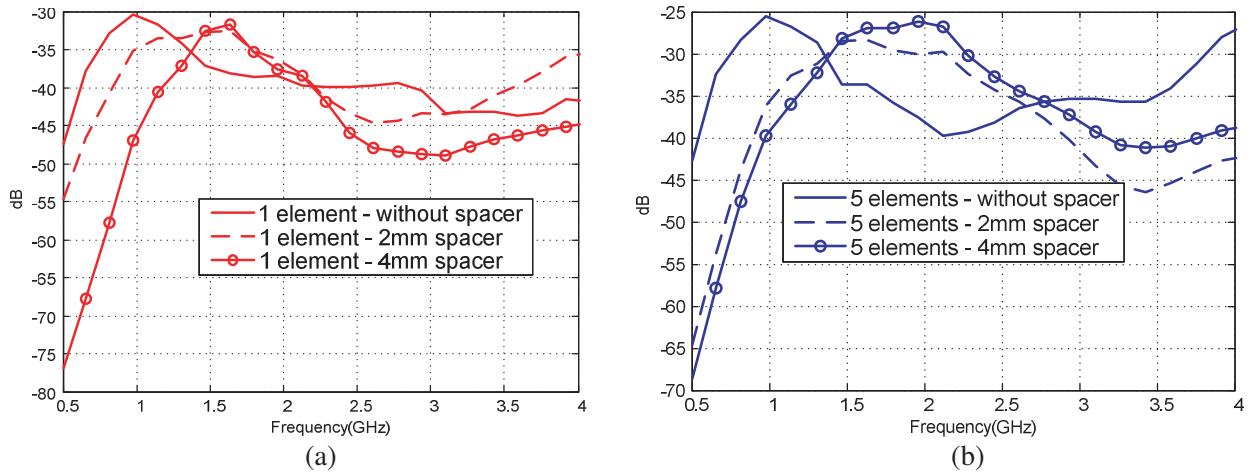
Figure 6. Comparison of FSS structure with (a) one and (b) five dipoles for different thickness of spacer between the FSS and the body.
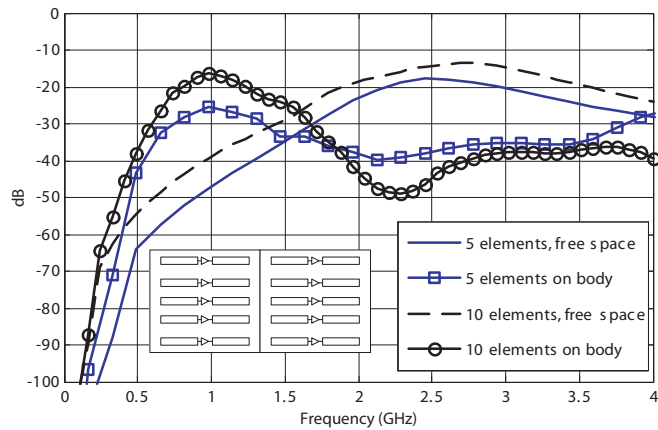

Figure 7. Simulated differential RCS of an FSS with 5 elements and 10 elements (distributed in two rows, see inset figure) in free space and on body.
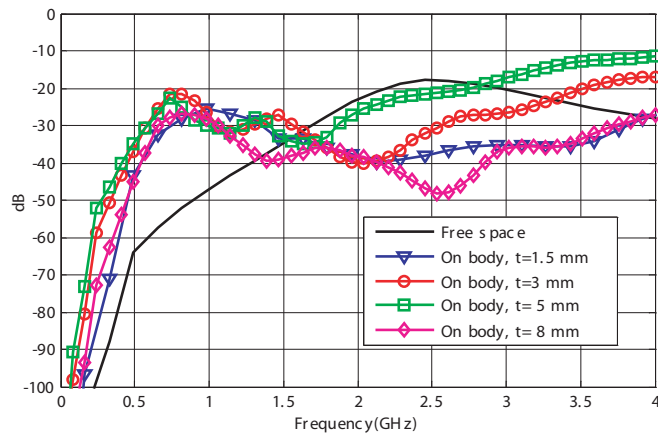

Figure 8. Simulated differential RCS of an FSS with 5 elements in free space and on body for different thicknesses of the fat layer (t).
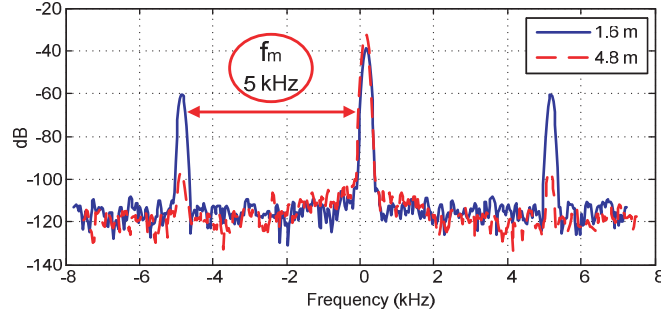
Figure 9. Measurement of the spectrum at 2.45 GHz (at 1.6 m solid line and 4.8 m dotted line).
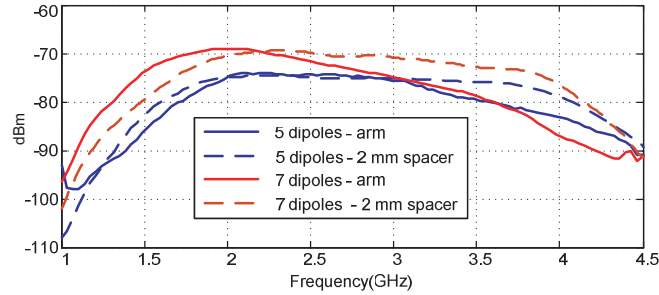

Figure 10. Comparison of FSS structure directly on contact with the arm and separated with a spacer of 2 mm [18].

dipoles is illuminated by a CW radar that transmits a power of 10 dBm at 2.45 GHz using a 8 dB gain antenna. Figure 9 shows the signal received at the spectrum analyzer (centred at 2.45 GHz) for two distances reader-tag, 1.6 m and 4.8 m. A strong central peak and two sideband peaks (f_m) are observed.

In order to characterize the frequency response of the modulated RCS, the FSS is illuminated in a range of frequencies, which varies from 1 to 4.5 GHz. Figure 10 shows the received power measured by the reader considering an FSS composed by 5 and 7 dipoles whose length is 25.6 mm. In this figure, two cases can be observed: the FSS directly on contact with the arm and separated with a spacer of 2 mm. The measurements are performed at a distance between the reader and the transponder of 1 m. The measured power is similar in the two cases, but when the FSS is on contact with the arm, the FSSs' spectral response is shifted (the bandpass is centred around 2 GHz), and the bandwidth is lower than the case when the FSS is separated with the spacer. The reason for this is the different permittivities and losses of the arm. The length of the dipole (L) can be redesigned considering the permittivity of the human body at the desired central frequency (f_c). The total effective permittivity (ε_{ref}) will be the average between the air and the effective permittivity of the body ($\varepsilon_{ref,body}$):

$$L \approx \frac{1}{2} \frac{c}{\sqrt{\varepsilon_{ref}} f_c} \tag{4}$$

$$\varepsilon_{ref} \approx \frac{1 + \varepsilon_{ref,body}}{2} \tag{5}$$

The effective permittivity of the FSS and the body can be obtained from Eqs. (4)–(5). Values of 8.6 and 16.1 have been found for the effective permittivity and effective permittivity of the body, respectively. It has been assumed that the resonance frequency is 2 GHz for the scenario in which the label is attached to the body.

In order to show the possibilities of the modulated FSS for wearable applications, some experiments have been performed. Two tags (Tag 1 and 2) are attached at different body locations. Each tag is composed by an FSS of 7 elements connected to different low-frequency oscillators that modulate the FSS at 5 kHz and 7 kHz, respectively. In a real application, each tag would be connected to different
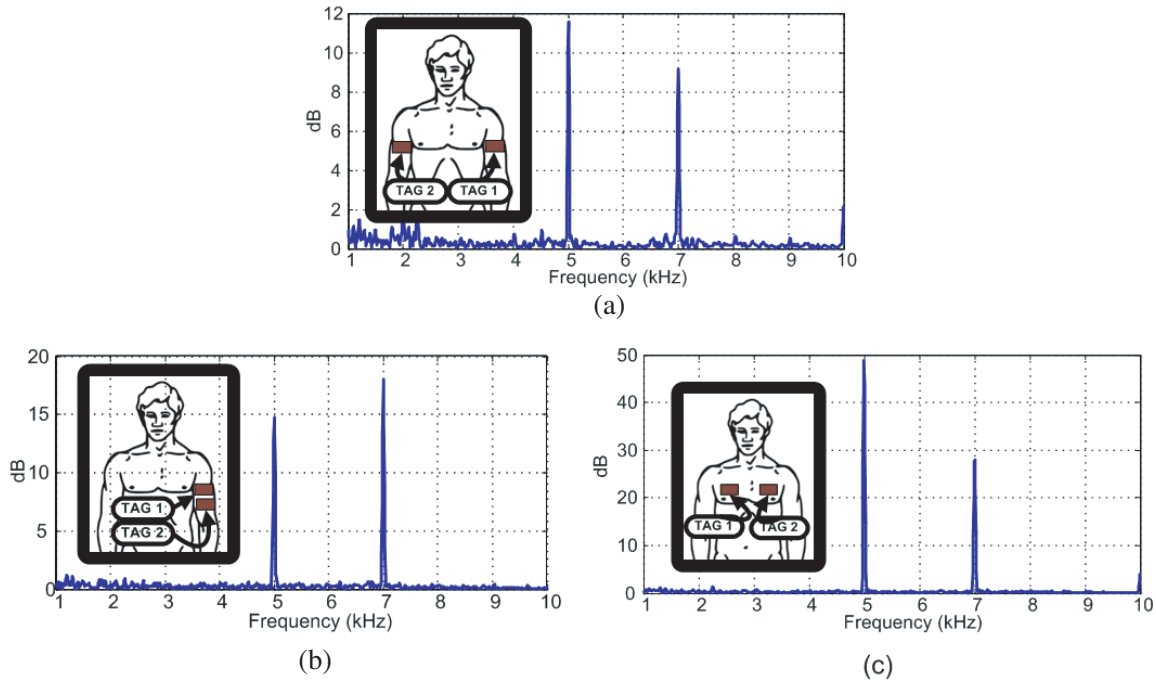
Figure 11. Received level at baseband after the A/D on the reader for two tags modulated at 5 kHz (Tag 1) and 7 kHz (Tag 2), respectively, at different body locations.

sensors. Each sensor can be simultaneously measured using different modulation frequencies. Due to the robustness of the FSS on body, the FSS can be connected near the sensor at different body locations. Figure 11 shows measurements at the output of the reader presented in [18] for a distance of 1 m. This reader is based on a homodyne radar where the baseband output of the mixer is sampled using an analogue-to-digital converter (ADC). The baseband spectrum can be obtained from Fourier transform of the sampled signal. Two peaks are shown corresponding to the modulation frequency of each tag. The relative amplitude of these peaks depends on the distance to the reader and propagation conditions.

4. CONCLUSIONS

In this paper, a modulated FSS for on-body applications is proposed. The communication between the transponder and the reader is based on the backscattering modulation of the FSSs' radar cross section (RCS). The simplest case is based on an FSS composed by loaded dipoles. Low-cost reverse biased varactors are used as switching elements in order to reduce the current consumption and to increase the battery lifetime, that is a key challenge in wearable devices. Due to limitations on the wearable devices size, finite FSS must be considered. Therefore, the effect of the number of elements and their dimensions have been studied. In addition, the detuning of the tag's response and the reduction of its radar cross section when it is closed to the body have also been studied. It has been demonstrated by means of simulations and measurements that a large bandwidth can be achieved. Therefore, the transponder is robust in front of a detuning response due to different electrical permittivities among persons or depending on whether the FSS is attached below or on the clothes. A reduction about 6 dB is observed when the FSS is on body compared with the FSS in free space.

REFERENCES

1. Montón, E., J. F. Hernandez, J. M. Blasco, T. Hervé, J. Micallef, I. Grech, A. Brincat, and V. Traver, "Body area network for wireless patient monitoring," *IET Commun.*, Vol. 2, No. 2, 215, 2008.

2. Rasyid, M. U. H. A., B. H. Lee, and A. Sudarsono, "Wireless body area network for monitoring body temperature, heart beat and oxygen in blood," *2015 International Seminar on Intelligent Technology and Its Applications (ISITIA)*, 95–98, 2015.

3. Movassaghi, S., M. Abolhasan, J. Lipman, D. Smith, and A. Jamalipour, "Wireless body area networks: A survey," *IEEE Commun. Surv. Tutor.*, Vol. 16, No. 3, 1658–1686, 2014.

4. Hoang, D. C., Y. K. Tan, H. B. Chng, and S. K. Panda, "Thermal energy harvesting from human warmth for wireless body area network in medical healthcare system," *2009 International Conference on Power Electronics and Drive Systems (PEDS)*, 1277–1282, 2009.

5. Barroca, N., H. M. Saraiva, P. T. Gouveia, J. Tavares, L. M. Borges, F. J. Velez, C. Loss, R. Salvado, P. Pinho, R. Gonçalves, N. BorgesCarvalho, R. Chavé-Santiago, and I. Balasingham, "Antennas and circuits for ambient RF energy harvesting in wireless body area networks," *2013 IEEE 24th Annual International Symposium on Personal, Indoor, and Mobile Radio Communications (PIMRC)*, 532–537, 2013.

6. Marrocco, G., "Pervasive electromagnetics: Sensing paradigms by passive RFID technology," *IEEE Wirel. Commun.*, Vol. 17, No. 6, 10–17, Dec. 2010.

7. Merilampi, S., P. Ruuskanen, T. Björninen, L. Ukkonen, and L. Sydänheimo, "Printed passive UHF RFID tags as wearable strain sensors," *2010 3rd International Symposium on Applied Sciences in Biomedical and Communication Technologies (ISABEL 2010)*, 1–5, 2010.

8. Amendola, S., R. Lodato, S. Manzari, C. Occhiuzzi, and G. Marrocco, "RFID technology for IoT-based personal healthcare in smart spaces," *IEEE Internet Things J.*, Vol. 1, No. 2, 144–152, Apr. 2014.

9. Rais, N. H. M., P. J. Soh, F. Malek, S. Ahmad, N. B. M. Hashim, and P. S. Hall, "A review of wearable antenna," *Antennas Propagation Conference, 2009, LAPC 2009, Loughborough*, 225–228, 2009.

10. Grosinger, J. and M. Fischer, "Evaluating on-body RFID systems at 900 MHz and 2.45 GHz," *2012 Fourth International EURASIP Workshop on RFID Technology (EURASIP RFID)*, 52–58, 2012.

11. Ziai, M. A. and J. C. Batchelor, "Temporary on-skin passive UHF RFID transfer tag," *IEEE Trans. Antennas Propag.*, Vol. 59, No. 10, 3565–3571, Oct. 2011.

12. Occhiuzzi, C., A. Ajovalasit, M. A. Sabatino, C. Dispenza, and G. Marrocco, "RFID epidermal sensor including hydrogel membranes for wound monitoring and healing," *2015 IEEE International Conference on RFID (RFID)*, 182–188, 2015.

13. Munk, B. A., R. G. Kouyoumjian, and L. Peters, Jr., "Reflection properties of periodic surfaces of loaded dipoles," *IEEE Trans. on Antennas Propag.*, Vol. 19, No. 5, 612–617, 1971.

14. Che, Y., X. Hou, and Z. Gao, "A tunable miniaturized-element frequency selective surfaces without bias network," *2011 IEEE International Conference on Microwave Technology & Computational Electromagnetics (ICMTCE)*, 70–73, 2011.

15. Lorenzo, J., A. Lazaro, D. Girbau, and R. Villarino, "Backscatter transponder based on frequency selective surface for FMCW radar applications," *Radioengineering*, 2014.

16. Lazaro, A., A. Ramos, D. Girbau, and R. Villarino, "A novel UWB RFID tag using active frequency selective surface," *IEEE Trans. on Antennas Propag.*, Vol. 61, No. 3, 1155–1165, 2013.

17. Thornton, J. and D. J. Edwards, "Range measurement using modulated retro-reflectors in FM radar system," *IEEE Microw. Guid. Wave Lett.*, Vol. 10, No. 9, 380–382, 2000.

18. Lorenzo, J., A. Lazaro, R. Villarino, and D. Girbau, "Modulated frequency selective surfaces for wearable RFID and sensor applications," *IEEE Trans. Antennas Propag.*, Vol. 64, No. 10, 4447–4456, Oct. 2016.

19. Collin, R. E. and F. J. Zucker, Ed., *The Receiving Antenna, Antenna Theory 1*, McGraw-Hill, New York, NY, USA, 1969.

20. Green, R. B., "The general theory of antenna scattering," Rep. 1223-17, ElectroScience Laboratory, Columbus, OH, 1963.

21. Nikitin, P. V., K. S. Rao, S. F. Lam, V. Pillai, R. Martinez, and H. Heinrich, "Power reflection coefficient analysis for complex impedances in RFID tag design," *IEEE Trans. Microw. Theory Tech.*, Vol. 53, No. 9, 2721–2725, 2005.

22. Gabriel, S., R. W. Lau, and C. Gabriel, "The dielectric properties of biological tissues: I. Literature survey," *Phys. Med. Biol.*, Vol. 41, No. 223, I-2249, 1996.

23. Gabriel, S., R. W. Lau, and C. Gabriel, "The dielectric properties of biological tissues: II. Measurements in the frequency range 10 Hz to 20 GHz," *Phys. Med. Biol.*, Vol. 41, No. 11, 2251, 1996.

24. Tsai, M.-C., C.-W. Chiu, H.-C. Wang, and T.-F. Wu, "Inductively coupled loop antenna design for UHF RFID on-body applications," *Progress In Electromagnetics Research*, Vol. 143, 315–330, 2013.